

# The additive function of *YIGE2* and *YIGE1* in regulating maize ear length

Yu Liu<sup>1,2,†</sup>, Huinan Li<sup>1,2,†</sup>, Jie Liu<sup>3</sup>, Yuebin Wang<sup>1,2</sup>, Chenglin Jiang<sup>1,2</sup>, Ziqi Zhou<sup>1,2</sup>, Lin Zhuo<sup>1,2</sup>, Wenqiang Li<sup>1,2</sup>, Alisdair R. Fernie<sup>4</sup> , David Jackson<sup>5</sup>, Jianbing Yan<sup>1,2,3</sup>  and Yun Luo<sup>1,2,\*</sup> 

<sup>1</sup>National Key Laboratory of Crop Genetic Improvement, Huazhong Agricultural University, Wuhan 430070, China,

<sup>2</sup>Hubei Hongshan Laboratory, Wuhan 430070, China,

<sup>3</sup>Yazhouwan National Laboratory, Sanya 572024, China,

<sup>4</sup>Department of Molecular Physiology, Max-Planck-Institute of Molecular Plant Physiology, Potsdam-Golm 14476 Germany, and

<sup>5</sup>Cold Spring Harbor Laboratory, Cold Spring Harbor, New York 11724, USA

Received 7 February 2024; revised 6 May 2024; accepted 10 May 2024.

\*For correspondence (e-mail [yunluo@mail.hzau.edu.cn](mailto:yunluo@mail.hzau.edu.cn)).

†These authors contributed equally to this work.

## SUMMARY

Ear length (EL) is a key trait that greatly contributes to yield in maize. Although dozens of EL quantitative trait loci have been mapped, very few causal genes have been cloned, and the molecular mechanisms remain largely unknown. Our previous study showed that *YIGE1* is involved in sugar and auxin pathways to regulate ear inflorescence meristem (IM) development and thus affects EL in maize. Here, we reveal that *YIGE2*, the paralog of *YIGE1*, regulates maize ear development and EL through auxin pathway. Knockout of *YIGE2* causes a significant decrease of auxin level, IM length, floret number, EL, and grain yield. *yige1 yige2* double mutants had even shorter IM and ears implying that these two genes redundantly regulate IM development and EL. The genes controlling auxin levels are differential expressed in *yige1 yige2* double mutants, leading to lower auxin level. These results elucidated the critical role of *YIGE2* and the redundancy between *YIGE2* and *YIGE1* in maize ear development, providing a new genetic resource for maize yield improvement.

**Keywords:** auxin, ear length, inflorescence meristem, maize, *YIGE1*/ *YIGE2*.

## INTRODUCTION

Maize (*Zea mays* L.) is one of the most productive cereal crops and plays a critical role in supporting the growing world population (Hawkins et al., 2013). Longer ears afford more space for kernel development, resulting in a higher kernel number per row (KNPR) and consequently an elevated grain yield (Huo et al., 2016; Jia et al., 2020; Liu et al., 2021). Hundreds of ear length (EL) quantitative trait loci (QTL) have been mapped in maize (Li et al., 2018; Xiao et al., 2016; Yi et al., 2019), but only few causal genes have been cloned and studied in detail (Jia et al., 2020; Luo et al., 2022; Ning et al., 2021; Pei et al., 2022). A serine/threonine protein kinase encoded by *KERNEL NUMBER ROW6* (*KNR6*), phosphorylates an auxin regulating factor GTPase-activating protein (AGAP), and functions in auxin-dependent inflorescence development to increase grain yield by increasing floret number, EL, and KNPR (Jia et al., 2020). Another EL gene, *ZmACO2*, which encodes 1-aminocyclopropane-1-carboxylate oxidase2 (ACO2) is involved in ethylene biosynthesis. Knockout of *ZmACO2*

reduces ethylene production in developing ears, leading to longer ears and higher grain yield (Ning et al., 2021). Moreover, *EAR APICAL DEGENERATION1* (*EAD1*) encodes an aluminum-activated malate transporter and plays an essential role in regulating maize ear development and EL by transporting malate to the immature ear tip through xylem vessels (Pei et al., 2022). These studies highlight the complexity of the genetic basis underlying EL and grain yield, both of which are insufficiently understood.

The duplicate *SBP*-box transcription factors genes *Unbranched2* (*UB2*), *UB3*, and *Tasselsheath4* (*TSH4*), redundantly regulated multiple agronomic traits including plant height (PH), tassel branch number (TBN), and kernel row number (KRN). Mutations in either *ub2*, *ub3*, or *tsh4* result in a modest reduction in PH, TBN, and an elevation in KRN. Disruption of two or more genes in the double and triple mutants leads to much severe decrease in PH, TBN, and increase in KRN (Chuck et al., 2014; Kong et al., 2022). The *APETALA2* (*AP2*)-like genes *indeterminate spikelet1* (*ids1*) and *sister of indeterminate spikelet1* (*sid1*) play

multiple roles in maize inflorescence architecture. *sid1* and *ids1* single mutants were phenotypically normal of inflorescence architecture. *sid1 ids1* double mutants had fewer branches and often had bare rachis in place of the missing rows (Chuck et al., 1998, 2008). *AUXIN/INDOLE-3-ACETIC ACID (AUX/IAA)*-related genes *BARREN INFLORESCENCE1 (BIF1)* and *BARREN INFLORESCENCE4 (BIF4)* regulate inflorescence axillary meristem initiation and determinacy. *bif1* and *bif4* mutants had reduced number of branches and spikelets, shortened ear with disorganized kernel rows. And these defects were more pronounced in *bif1 bif4* double mutants (Galli et al., 2015). These studies shed lights on the conservation and redundancy of the function of homologous genes.

Previously, we cloned another EL QTL, *YIGE1*, which positively regulates EL and grain yield by affecting inflorescence meristem (IM) length and floret number through sugar and auxin pathways (Luo et al., 2022). Here, we reported a new EL gene, *YIGE2*, a paralog of *YIGE1*. *YIGE2* knockout lines displayed a decreased EL, KNPR, and ear weight without changes of flowering or plant architecture traits. Loss-of-function mutation of *YIGE2* lead to significant decrease of auxin level. Double mutation of *yige1 yige2* dramatically enhanced the EL and the level of auxin. Our results showed that *YIGE2* plays a redundant role with *YIGE1* in regulating EL. The identification of *YIGE2* and its relationship with *YIGE1* expand our knowledge of the molecular mechanism of maize ear development.

## RESULTS

### *YIGE2* regulates maize EL

*YIGE1*, encoding a cytoplasm-localized unknown protein, positively regulates maize EL and grain yield without affecting plant growth (Luo et al., 2022). Its homolog, *HCF243*, in *Arabidopsis (Arabidopsis thaliana)*, was reported to encode a chloroplast localized protein and involved in D1 protein stability of the photosystem II complex, and its mutants had higher chlorophyll fluorescence with pale rosette leaves (Zhang et al., 2011). Therefore, *YIGE1* showed functional divergence in maize and *Arabidopsis* (Luo et al., 2022). *YIGE1* has one paralog, *Zm00001d047617*, which we named *YIGE2*. *YIGE2* shows 84.26% amino acid identity to *YIGE1* (Figure S1). The main sequence difference between them is an extra 262 amino acids at the N terminus of *YIGE2*. Despite this sequence difference, they exhibit similar expression patterns. Both of them are constitutively expressed and show highest expression level in developing ears (Figure 1A). In addition, *YIGE2* was also localized in the cytoplasm (Figure 1B; Figure S2), which is similar to the cellular localization of *YIGE1* (Luo et al., 2022). These results indicated the redundancy of *YIGE2* and *YIGE1* and also suggested that *YIGE2* may be involved in regulating ear development.

To determine the function of *YIGE2*, we used CRISPR-Cas9 to edit *YIGE2* and obtained three independent transgenic lines (*yige2-cr1*, *-cr2*, and *-cr3*). All three lines harbored one or more insertions/deletions that caused frame shift or early termination (Figure 1C). All three loss-of-function lines had a decrease in EL by ~4.0–10.2%, KNPR by ~6.4–11.0%, and ear weight by ~11.7–22.9% when comparing with their corresponding wild-type (WT) siblings across multiple environments (Figure 1D–G; Figure S3). Moreover, we measured a set of agronomic traits, including flowering time, PH, ear height, ear leaf length and width, tassel main axis length, TBN, and KRN. Compared to WT, *yige2* knockout lines had no significant difference in flowering time, KRN, and plant architecture traits (Figures S4–S6). These results confirmed the function of *YIGE2* in regulating EL, KNPR, and grain yield without the penalty of other agronomic traits, and also highlighted the great potential of *YIGE2* for maize improvement.

### *YIGE2* regulates IM size and florets number

During the reproductive stage, the ear IM forms spikelet pair meristems that develop into spikelet meristems and floral meristems (Vollbrecht & Schmidt, 2009). A larger IM provides more space for floral meristem development, contributing to EL through a higher floret number (Jia et al., 2020; Luo et al., 2022). To investigate the mechanism of *YIGE2* in regulating ear development, we used scanning electron microscope to visualize the developing inflorescence. After measuring the length of IM in 3–4 mm developing ears and counting the floret number before pollination, we found that *yige2-cr3* knockout lines had a significant shorter IMs, reduced floret number per row, and shorter EL when comparing with WT (Figure 2). There was no significant difference of the number of kernels developed from florets after pollination between *yige2-cr3* and WT (Figures 1E and 2C). These findings indicate that *YIGE2* controls ear development through the regulation of IM and floret number.

### *YIGE2* plays a redundant role with *YIGE1*

To further elucidate the genetic relationship between *YIGE2* and *YIGE1*, we generated double-mutants through crossing *yige2* with *yige1*. In the F<sub>2</sub>, the mutants segregated according to Mendel's laws of independent assortment and segregation (Figure S7), indicating that these two genes are inherited independently. As expected, the double mutants had a more pronounced phenotype with an even shorter IM comparing with either *yige2* or *yige1* (Figure 3A,B). Consequently, much shorter EL and less KNPR were observed in double mutants than that of single mutants (Figure 3C–E; Figure S8). In addition, there was no significant difference in KRN between WT, *yige1*, *yige2*, and *yige1 yige2* (Figure 3F). In summary, these results confirmed that

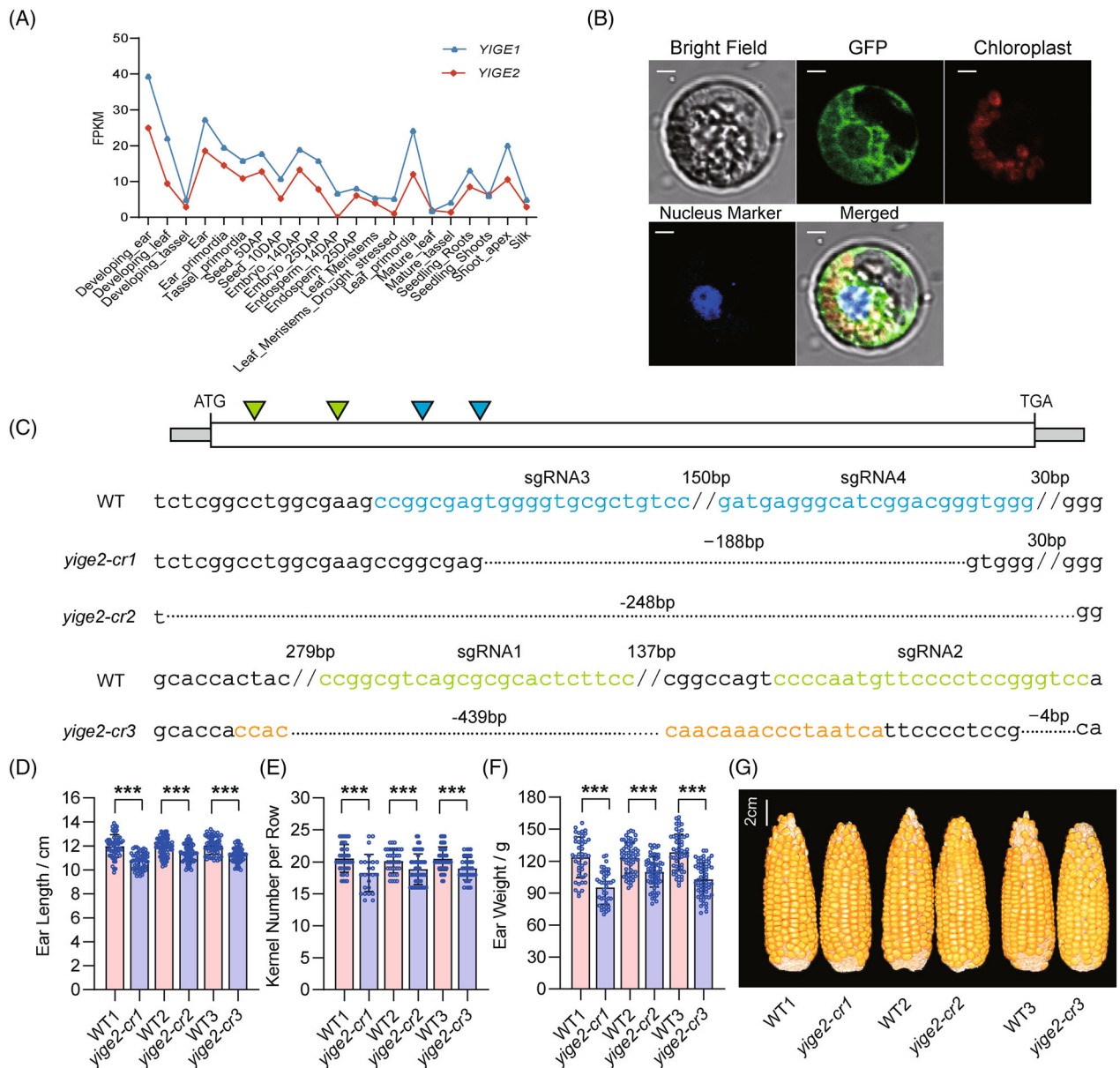


**Figure 1.** *YIGE2* controls ear length and grain yield.

(A) Expression pattern of *YIGE2* and *YIGE1*. The data is from MaizeGDB (<https://maizegdb.org/>).

(B) The subcellular localization of *YIGE2*. DAPI was used to stain nuclear. *YIGE1*-GFP was detected in the cytoplasm of maize protoplasts.

(C) The gene structure and three exon-edited alleles of *YIGE2*. The green and blue triangles show the sgRNAs target sites on *YIGE2*. The sgRNAs sequences are marked in green and blue. The lengths of deletions are indicated by numbers. The insertions are marked in orange.

(D–G) Comparison of ear length (D, G), kernel number per row (E), ear weight (F) between wild type and *YIGE2* knockout lines. The data are presented as means  $\pm$  SD, and the blue dots represent the phenotype values of measured samples in (D–F). Level of significance is determined by a one-way ANOVA analysis. \*\*\**P* < 0.001. Scale bar = 5  $\mu$ m in (B) and 2 cm in (G).

*YIGE2* had redundant role with *YIGE1* in regulating maize ear development.

### ***YIGE2* and *YIGE1* are involved in an auxin signaling pathway**

To identify the regulatory network in which *YIGE2* and *YIGE1* were involved, we conducted RNA-seq using ~2 mm

developing ears from WT, *yige1*, *yige2*, and *yige1 yige2*. Compared to WT, we identified 559 differentially expressed genes (DEGs) in *yige2* with 247 genes upregulated and 312 genes downregulated (Figure S9a). In *yige1*, 757 DEGs were detected with 376 genes upregulated and 381 genes downregulated (Figure S9b). Additionally, we detected 720 DEGs in *yige1 yige2* with 315 genes upregulated and 40

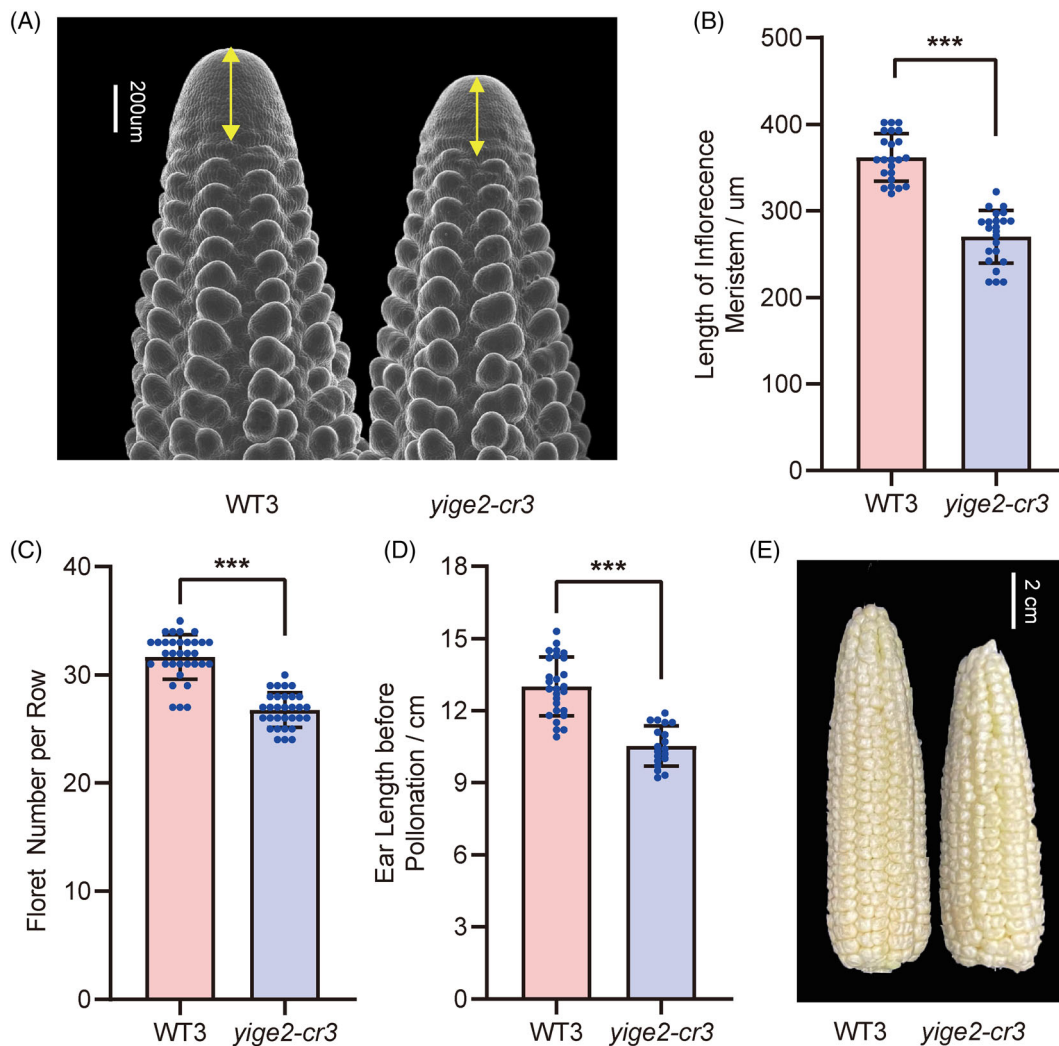


**Figure 2.** *YIGE2* regulates inflorescence meristem and floret production.

(A) Micrograph of 3–4 mm immature apical ears of wild type and *YIGE2* knockout lines. Yellow lines represent inflorescence meristem length. (B–E) Inflorescence meristem (IM) length (B), floret number per row (C) and ear length before pollination (D, E) of WT and *yige2-cr3*. Data in (B–D) are shown as the mean  $\pm$  SD. The significant differences are determined by one-way ANOVA analysis. Each blue dot indicates phenotype value of each sample in (B–D). \*\*\* $P < 0.001$ . Scale bar = 200  $\mu\text{m}$  in (A) and 2 cm in (E).

genes downregulated (Figure 4A). After performing gene ontology (GO) analysis, 26 GO terms were enriched in both single mutants and double mutant, including response to hormone, response to temperature stimulus, and response to abiotic stimulus (Figure 4B; Figure S9c–e). Hormones, especially auxin, play a crucial role in maize ear development (Gallavotti, 2013; Galli et al., 2015; Jia et al., 2020; Luo et al., 2022; McSteen et al., 2007; Ross et al., 2001; Zhao, 2010). Therefore, we primarily focused on the enriched GO item of response to hormone and identified several auxin-related genes, including *Zm00001d048709* encoding IAA biosynthesis I, *Zm00001d043660* encoding auxin efflux carrier family protein, *Zm00001d010697* encoding auxin-responsive GH3 family protein, and *Zm00001d032422* encoding auxin associated family

protein, which are differentially expressed in *yige1 yige2* (Figure 4C).

To further explore the connection between *YIGE2/YIGE1* and auxin, we next measured the auxin level via LC–MS/MS in 2–5 mm developing ears of WT, *yige1*, *yige2*, and *yige1 yige2*. There were no significant differences in the levels of 3-indoleacetonitrile, indole-3-carboxylic acid, and methyl indole-3-acetate when comparing mutants with WT (Figure S10). However, we observed significant differences in the levels of indole-3-acetic acid (IAA), indole-3-acetyl-L-aspartic acid (IAA-Asp), indole-3-acetyl glutamic acid, 2-oxindole-3-acetic acid (OxIAA), L-tryptophan, indole, and its precursor substance tryptamine (Figure 4D; Figure S10). Moreover, the reductions of IAA, IAA-Asp, and OxIAA content in *yige1 yige2* were greater

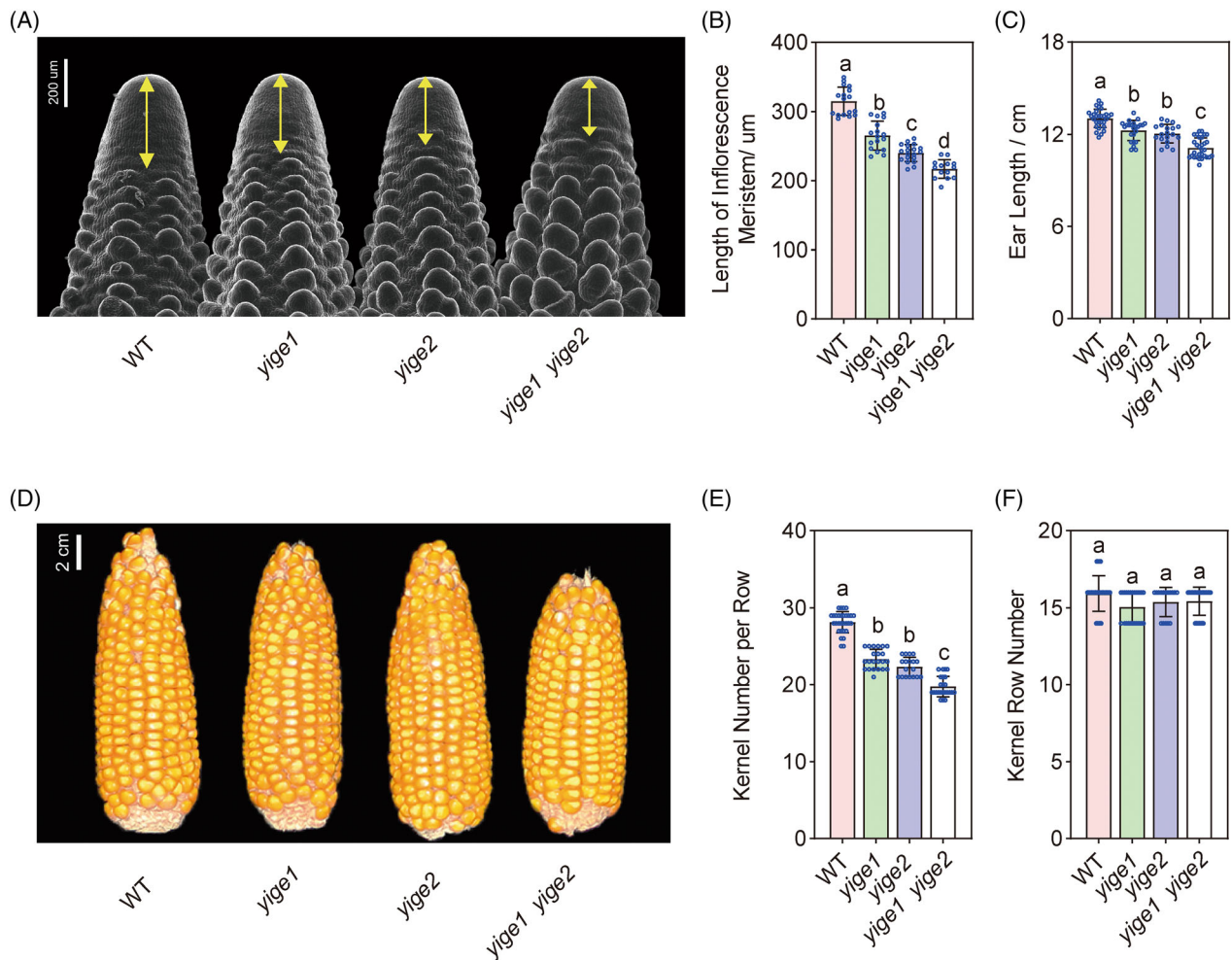


**Figure 3.** The redundancy between *YIGE2* and *YIGE1*.

(A, B) Micrograph of 3–4 mm immature apical ears and inflorescence meristem length (B) of wild type, *yige1*, *yige2*, and *yige1 yige2*. Yellow lines represent inflorescence meristem length in (A).

(C–F) The ear length (C, D), kernel number per row (E) and kernel row number (F) between wild type, *yige1*, *yige2*, and *yige1 yige2*. Data are shown as the mean  $\pm$  SD. The significant differences are determined by multiple comparisons and a,b,c,d indicate significant differences ( $P < 0.05$ ). Each blue dot in (B, C, E, F) indicates phenotype value of each sample. Scale bar = 200  $\mu\text{m}$  in (A) and 2 cm in (D).

relative to either *yige1* or *yige2* (Figure 4D). Taken together, our results suggested that both *YIGE2* and *YIGE1* participate in the regulation of auxin content (Figure 4E).

## DISCUSSION

Ear length plays an important role in maize grain yield (Xu et al., 2018; Zhou et al., 2018). Previous studies have shown that EL was affected by IM size, florets production, and floral fertility (Jia et al., 2020; Luo et al., 2022; Ning et al., 2021; Pei et al., 2022). *KNR6* and *YIGE1* enhanced EL and grain yield by raising IM size and floret production without altering floral fertility (Jia et al., 2020; Luo et al., 2022). By contrast, *ZmACO2* loss of function lines showed increased EL by promoting IM with more florets and enhanced floret fertility (Ning et al., 2021). Moreover, dysfunction of *EAD1* resulted in apical IM degeneration with SPMs/SMs collapsing

extending and deteriorating in  $\geq 20$  mm inflorescences, leading to the abortion of florets and ultimately a shorter EL (Pei et al., 2022). These studies highlighted the complexity of genetic bases and molecular mechanism of EL. In our current study, *YIGE2* knockout lines were found to have a shorter IM length and EL, lower FNPR, and similar floret fertility (Figures 1 and 2). In addition, *yige1 yige2* showed a more severe phenotype (Figure 3), suggesting that *YIGE2* plays a redundant role with *YIGE1* in regulation of maize.

*YIGE2/1* are expressed in multiple tissues, yet the knockout of *yige1* and *yige2* appears to specifically affect ear phenotypes. One plausible explanation for this observation is that *YIGE2/1* are expressed at higher levels in the developing ear compared to other tissues, which could contribute to its predominant effect on ear phenotypes upon knockout. Moreover, *YIGE2/1*, being a cytoplasmic

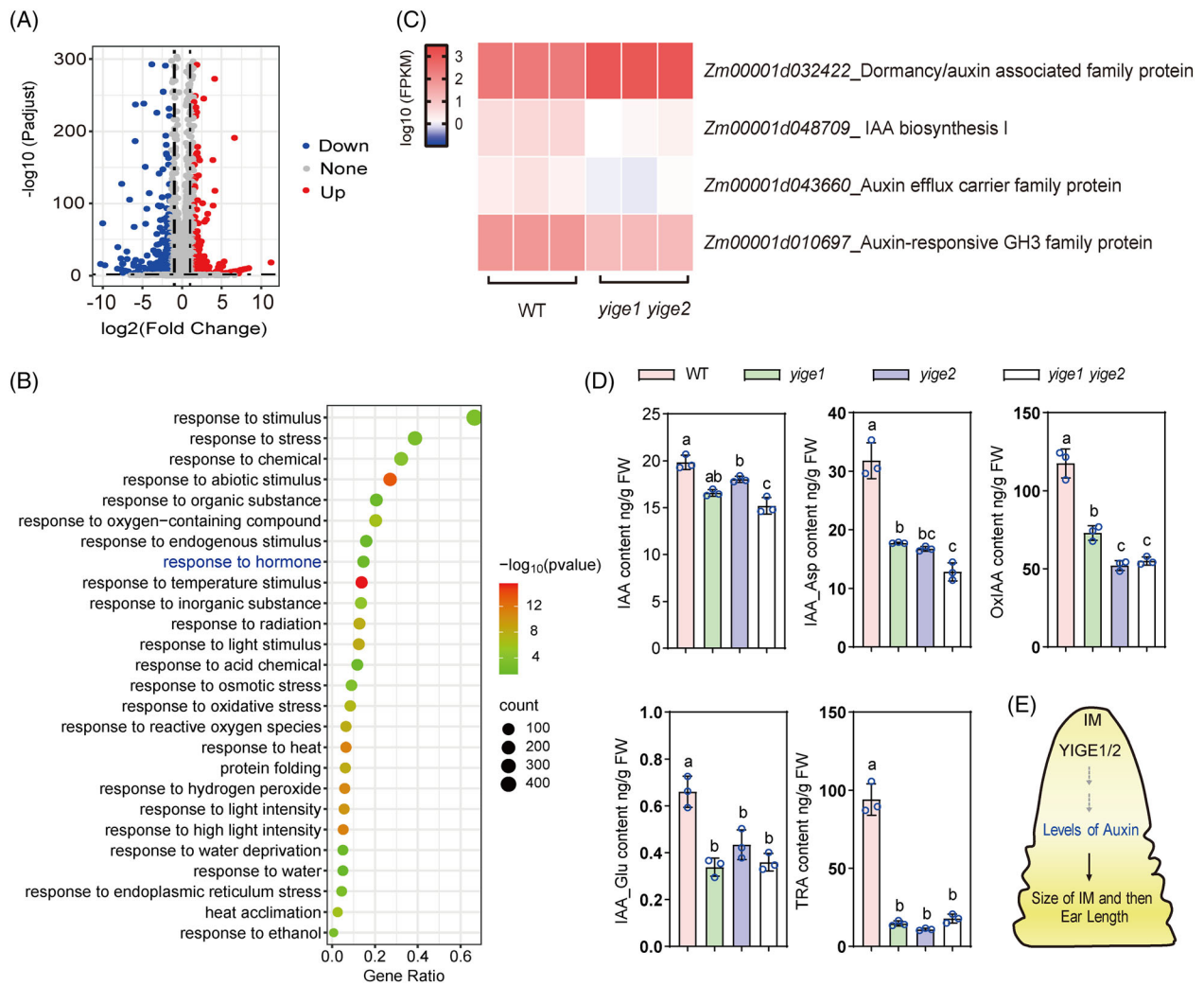


**Figure 4.** *YIGE1* and *YIGE2* affect EL through regulating auxin signaling.

(A) Differentially expressed genes between WT and *yige1 yige2*. Each dot represents a gene. Blue and red dots represented the downregulated and upregulated genes, respectively.

(B) Significantly enriched Gene Ontology items (false discovery rate <0.05) shared by single and double mutants.

(C) Auxin-related differentially expressed genes.

(D) Quantification of auxin in the developing ears of WT, *yige1*, *yige2* and *yige1 yige2*. Data are shown as the mean  $\pm$  SD. The significant differences are determined by multiple comparisons and a,b,c,d indicate significant differences ( $P < 0.05$ ). Each blue dots represent the phenotype value of each sample in (D).

(E) A proposed model to illustrate the regulatory pathway in which *YIGE2* and *YIGE1* are involved in.

protein, may not directly regulate gene expression at the transcriptional level. Instead, it is conceivable that *YIGE2/1* interacts with other proteins or forms complexes that play crucial roles in ear development. These interactions could involve signaling pathways, protein–protein interactions, or posttranslational modifications that specific to the ear tissue. To explore the interaction proteins with *YIGE2/1*, we identified 13 potential interaction proteins with *YIGE2/1* based on the published data (Han et al., 2023), and three was further selected for luciferase complementation assay in tobacco (Table S1). Unfortunately, none positive interaction was detected (Supplementary Fig. 11). Therefore, investigating the downstream targets or interacting

partners of *YIGE2/1* in the context of ear development will require more considerable future research effort.

Maize was an ancient tetraploidy and this polyploidy resulted in there are two duplicates (maize 1 and maize 2 subgenomes) of the current diploid maize genome (Salse et al., 2008; Wei et al., 2007). *YIGE1* is located in chromosome 1 and belongs to maize1 subgenome, while *YIGE2* is located in chromosome 9 and belongs to maize2 subgenome in modern maize (Schnable et al., 2011). Moreover, segments of *YIGE1* and *YIGE2* in maize blasted to the same sorghum chromosome1 (Schnable et al., 2011). These results indicated that the mechanisms of retaining the two genes is the ancient polyploidy. Moreover, the functional

redundancy of *YIGE1* and *YIGE2* can be protective, ensuring that loss of function in one gene does not result in a loss of the essential gene function in regulating maize ear development.

Moreover, we found that GO items of auxin pathway were significantly enriched in *yige1*, *yige2*, and *yige1 yige2* but not sugar pathway related GO items (Figure 4B; Figure S9). This is inconsistent with the findings in *YIGE1* overexpression materials (Luo et al., 2022). It may be attributed to the full-length coding sequence of *YIGE1* driven by the ubiquitin promoter in *YIGE1* overexpression lines, leading to some other effects associated with ectopic expression. Auxin plays a critical role in regulation of florets production on maize ear (Carraro et al., 2006; Jia et al., 2020; Luo et al., 2022; McSteen et al., 2007; Phillips et al., 2011), which is consistent with our observation that decreased auxin contents in *yige1*, *yige2* result in fewer floret number, shorter EL, and lower grain yield (Figures 2–4).

*YIGE1* underwent continuous selection, and the favorable allele was enriched during maize domestication and improvement (Luo et al., 2022). However, we did not find the evidence that *YIGE2* was under selection during maize domestication and improvement (Chen et al., 2022). We try to find the possible variations in *YIGE2* correlated to EL in 513 association mapping population and identified 57 single nucleotide polymorphisms (SNPs) in 1 kb promoter region and 88 SNPs in gene body region of *YIGE2* (Chen et al., 2022). However, no SNPs show significant correlation with EL. In addition, overexpression of *YIGE1* resulted in a higher EL and elevated grain yield. *YIGE2* and *YIGE1* exhibit conservation in regulation of maize ear development and grain yield (Figures 1–3). We speculated that higher expression level of *YIGE2* may increase EL and grain yield, similar with *YIGE1*. Therefore, it is promising to obtain longer ears and higher grain yield through enhancing the expression level of *YIGE2* via editing the promoter of *YIGE2* by CRISPR/Cas9 technology or overexpressing *YIGE2*. Moreover, further studies are required to reveal more precise details concerning the function of *YIGE1* and *YIGE2* as these will be helpful in understanding maize ear development as well as facilitating the genetic improvement of grain yield.

## MATERIALS AND METHODS

### Vector construction, genetic transformation, and identification of the transgenic maize

CRISPR/Cas9 was used to induce mutations in the *YIGE2* (*Zm00001d047617*) exon region. Single-guide RNAs (sgRNAs) were designed based on the B73 reference genome sequence using CRISPR-P webtool (Liu et al., 2017) (<http://crispr.hzau.edu.cn/CRISPR2/>). Four sgRNAs were selected, synthesized, and cloned into the pCPBZmUbi-hspCas9 binary vector following the manufacturer's recommended protocols (Li et al., 2017). Subsequently, the CRISPR-Cas9 plasmids were transformed into the inbred line KN5585 via *Agrobacterium*-mediated transformation at

Weimi Biotechnology in Jiangsu, China (Liu et al., 2020). Genomic editing of *YIGE2* was screened by PCR amplification and Sanger sequencing of the target regions. Cas9-negative edited plants underwent selfing for two generations before further phenotypic scoring. The edited lines were cultivated in JiLin, China (43.5° N, 124.82° E), and Hubei (Wuhan; 30.58° N, 114.31° E), China. The plants were grown in 2.5 m rows, spaced 0.5 m apart, with 11 individuals in each row. The sgRNAs and primers used for genotype of *YIGE2* are provided in Table S2.

### Double mutant analysis

The *yige1 yige2* double mutants were generated by crossing the *YIGE2-cr3* knockout lines to *YIGE1* knockout lines. For genotyping, leaf tissue was collected from 4-week-old plants, and DNA was extracted according to a modified CTAB protocol. PCR was carried out to genotype the plants using primers CR8490-F (5' ATGATGGGGGATGTGGAGG 3') and CR8490-R (5' TCGCTCCGC AGACTTTGT 3') for *YIGE1*, and using primers HZY7-F (5' GGGCC ATGCTACACAATTAC 3') and HZY7-R (5' CACCTCCACTTCCCC TACCA 3') for *YIGE2*, respectively. The *yige1 yige2* double mutants were easily identified based on the genotype. For analysis of EL, KNPR, and ear weight, >30 plants of each genetic class were analyzed.

### Phenotype measurement and data analysis

By 40 days of plants growth, wild type, *yige1*, *yige2*, and *yige1 yige2* double mutants ~4 mm developing ear were collected and taken pictures using a stereomicroscope (Olympus; SZX10; Tokyo, Japan). Next, the size of IM was measured using ImageJ (Schindelin et al., 2015) and analyzed by Excell 2020. Moreover, we collected maize ears before and after pollination from WT and *yige2* knockout lines, and counted KNPR and measured EL with ruler. Progeny tests were performed by the Student's test.

### Subcellular localization of YIGE2

The full-length *YIGE2* coding sequence was amplified from B73 cDNA and cloned downstream of the *CaMV35S* promoter in the pCAMBIA1302 vector that carried GFP. A pCAMBIA1302-35S: *YIGE2*-GFP construct was introduced into maize protoplasts as described previously (Yoo et al., 2007). The GFP signals were detected using a FV1200 Laser Scanning Microscope (Olympus Corporation). The primers of cloning full-length *YIGE2* coding sequence are listed in Table S2.

### RNA-seq

Total RNA was extracted from ~2 mm developing ears of WT, *yige1*, *yige2*, *yige1 yige2* double mutants using a Quick RNA Isolation Kit (Huayueyang Biotechnology Co., Ltd. Beijing, China). For RNA-seq, three biological replicates were performed for each sample. The RNA libraries were prepared using commercial Illumina library preparation kits (TruSeq Stranded mRNA LT-SetA. RS-122-1201) and subsequently sequenced following the HiSeq X-Ten protocols. Trimmomatic (v0.36) was employed to filter out lower-quality sequencing reads (Bolger et al., 2014). RSEM-1.3.0 was utilized for aligning RNA-seq reads to the B73 v4 reference genome, and gene expression levels were estimated using default parameters (Li & Dewey, 2011).

### Detection the levels of auxin in developing ear

Fresh immature ears (2–5 mm) from WT, *yige1*, *yige2* and *yige1 yige2* double mutants with at least three biological replicates were

obtained and saved in liquid nitrogen. Then auxin contents were quantified by MetWare (<http://www.metware.cn/>). Approximately 50 mg of powder was dissolved in 1 ml mixture of methanol, water and formic acid (15:4:1, v/v/v), and 10  $\mu$ l of the internal standard mixed solution (100 ng ml<sup>-1</sup>) was added to the extract as internal standards (IS) for the quantification. The resulting mixture was vortexed for 10 min at 4°C. Following centrifugation at 18 400 g at 4°C, the supernatant was carefully transferred to a clean plastic microtube and subjected to evaporation until dryness. The dried samples were reconstituted in 100  $\mu$ l of 80% methanol (v/v), filtered through a 0.22  $\mu$ m membrane and subsequently transferred to sample vials for subsequent LC-MS/MS analysis (Floková et al., 2014; Li et al., 2016; Šimura et al., 2018) in an UPLC-ESI-MS/MS system consisting of UPLC, ExionL™ AD (<https://sciex.com.cn/>) and MS, Applied Biosystems 6500 Triple Quadrupole (<https://sciex.com.cn/>). The auxin levels were assessed by comparing the response of the IS added during extraction to the developing ear sample components.

### AUTHOR CONTRIBUTIONS

YLuo and JY designed and supervised this study. YLuo, YLiu and HL performed the field trials, validation of gene function and gene expression analysis. CJ constructed the transgenic vector. YLuo, JY, AF, JL, and DJ wrote and revised the manuscript. All the authors read and approved the paper.

### ACKNOWLEDGEMENTS

This research was supported by funding from the National Key Research and Development Program of China (2022YFD1201500), the National Natural Science Foundation of China (U1901201 and 32301840), the China Postdoctoral Science Foundation (2023M731239), and Hubei Provincial Natural Science Foundation of China (2023AFB261).

### CONFLICT OF INTEREST

The authors declare no competing financial interests.

### SUPPORTING INFORMATION

Additional Supporting Information may be found in the online version of this article.

**Figure S1.** Amino acid sequence alignment of YIGE1 and YIGE2.

**Figure S2.** The subcellular localization of YIGE2.

**Figure S3.** Transgenic validation of YIGE2 in JiLin, China.

**Figure S4.** Flowering traits and plant architecture of wild type and *yige2-cr1* knockout lines.

**Figure S5.** Flowering traits and plant architecture of wild type and *yige2-cr3* knockout lines.

**Figure S6.** Comparison of kernel row number between wild type and *yige2-cr3* knockout lines.

**Figure S7.** Selecting double-mutant materials in the F<sub>2</sub> segregating population.

**Figure S8.** Comparison of ear length between wild type, *yige1*, *yige2*, and *yige1; yige2* double mutant.

**Figure S9.** RNA-seq analysis in WT, *yige1*, *yige2*, and *yige1 yige2* double mutants.

**Figure S10.** Auxin content in the developing ear of WT, *yige1*, *yige2*, and *yige1 yige2* double mutants.

**Figure S11.** Analysis of protein interaction between YIGE2/1 and Zm00001d047757, Zm00001d049294, and Zm00001d049346.

**Table S1.** The potential interaction proteins of YIGE2/1.

**Table S2.** Primers are used in the experiment.

### OPEN RESEARCH BADGES



This article has earned an Open Data badge for making publicly available the digitally-shareable data necessary to reproduce the reported results. The RNA-seq data from this study have been deposited in CNGBdb (<https://db.cngb.org/>), and under project accession code CNP0005548. And the full genomic sequence of YIGE2 can be found in GenBank (accession no. BankIt2819411 Seq1PP693109).

### DATA AVAILABILITY STATEMENT

The RNA-seq data from this study have been deposited in CNGBdb (<https://db.cngb.org/>), and under project accession code CNP0005548. And the full genomic sequence of YIGE2 can be found in GenBank (accession no. BankIt2819411 Seq1PP693109).

### REFERENCES

- Bolger, A.M., Lohse, M. & Usadel, B.** (2014) Trimmomatic: a flexible trimmer for Illumina sequence data. *Bioinformatics*, **30**, 2114–2120.
- Carraro, N., Forestan, C., Canova, S., Traas, J. & Varotto, S.** (2006) *ZmPIN1a* and *ZmPIN1b* encode two novel putative candidates for polar auxin transport and plant architecture determination of maize. *Plant Physiology*, **142**, 254–264.
- Chen, W., Chen, L., Zhang, X., Yang, N., Guo, J., Wang, M. et al.** (2022) Convergent selection of a WD40 protein that enhances grain yield in maize and rice. *Science*, **375**, eabg7985.
- Chuck, G., Meeley, R. & Hake, S.** (2008) Floral meristem initiation and meristem cell fate are regulated by the maize AP2 genes *ids1* and *sid1*. *Development*, **135**, 3013–3019.
- Chuck, G., Meeley, R.B. & Hake, S.** (1998) The control of maize spikelet meristem fate by the APETALA2-like gene *indeterminate spikelet1*. *Genes & Development*, **12**, 1145–1154.
- Chuck, G.S., Brown, P.J., Meeley, R. & Hake, S.** (2014) Maize SBP-box transcription factors *unbranched2* and *unbranched3* affect yield traits by regulating the rate of lateral primordia initiation. *Proceedings of the National Academy of Sciences of the United States of America*, **111**, 18775–18780.
- Floková, K., Tarkowská, D., Miersch, O., Strnad, M., Wasternack, C. & Novák, O.** (2014) UHPLC-MS/MS based target profiling of stress-induced phytohormones. *Phytochemistry*, **105**, 147–157.
- Gallavotti, A.** (2013) The role of auxin in shaping shoot architecture. *Journal of Experimental Botany*, **64**, 2593–2608.
- Galli, M., Liu, Q., Moss, B.L., Malcomber, S., Li, W., Gaines, C. et al.** (2015) Auxin signaling modules regulate maize inflorescence architecture. *Proceedings of the National Academy of Sciences of the United States of America*, **112**, 13372–13377.
- Han, L., Zhong, W., Qian, J., Jin, M., Tian, P., Zhu, W. et al.** (2023) A multi-omics integrative network map of maize. *Nature Genetics*, **55**, 144–153.
- Hawkins, E., Fricker, T.E., Challinor, A.J., Ferro, C.A., Ho, C.K. & Osborne, T.M.** (2013) Increasing influence of heat stress on French maize yields from the 1960s to the 2030s. *Global Change Biology*, **19**, 937–947.
- Huo, D., Ning, Q., Shen, X., Liu, L. & Zhang, Z.** (2016) QTL mapping of kernel number-related traits and validation of one major QTL for ear length in maize. *PLoS One*, **11**, e0155506.
- Jia, H., Li, M., Li, W., Liu, L., Jian, Y., Yang, Z. et al.** (2020) A serine/threonine protein kinase encoding gene *KERNEL NUMBER PER ROW6* regulates maize grain yield. *Nature Communications*, **11**, 988.
- Kong, D., Li, C., Xue, W., Wei, H., Ding, H., Hu, G. et al.** (2022) UB2/UB3/TSH4-anchored transcriptional networks regulate early maize

- inflorescence development in response to simulated shade. *The Plant Cell*, **35**, 717–737.
- Li, B. & Dewey, C.N. (2011) RSEM: accurate transcript quantification from RNA-Seq data with or without a reference genome. *BMC Bioinformatics*, **12**, 323.
- Li, C., Liu, C., Qi, X., Wu, Y., Fei, X., Mao, L. *et al.* (2017) RNA-guided Cas9 as an in vivo desired-target mutator in maize. *Plant Biotechnology Journal*, **15**, 1566–1576.
- Li, M., Zhong, W., Yang, F. & Zhang, Z. (2018) Genetic and molecular mechanisms of quantitative trait loci controlling maize inflorescence architecture. *Plant & Cell Physiology*, **59**, 448–457.
- Li, Y., Zhou, C., Yan, X., Zhang, J. & Xu, J. (2016) Simultaneous analysis of ten phytohormones in *Sargassum horneri* by high-performance liquid chromatography with electrospray ionization tandem mass spectrometry. *Journal of Separation Science*, **39**, 1804–1813.
- Liu, H., Ding, Y., Zhou, Y., Jin, W., Xie, K. & Chen, L.L. (2017) CRISPR-P 2.0: an improved CRISPR-Cas9 tool for genome editing in plants. *Molecular Plant*, **10**, 530–532.
- Liu, H.J., Jian, L., Xu, J., Zhang, Q., Zhang, M., Jin, M. *et al.* (2020) High-throughput CRISPR/Cas9 mutagenesis streamlines trait gene identification in maize. *The Plant Cell*, **32**, 1397–1413.
- Liu, M., He, W., Zhang, A., Zhang, L., Sun, D., Gao, Y. *et al.* (2021) Genetic analysis of maize shank length by QTL mapping in three recombinant inbred line populations. *Plant Science: An International Journal of Experimental Plant Biology*, **303**, 110767.
- Luo, Y., Zhang, M., Liu, Y., Liu, J., Li, W., Chen, G. *et al.* (2022) Genetic variation in *YIGE1* contributes to ear length and grain yield in maize. *New Phytologist*, **234**, 513–526.
- McSteen, P., Malcomber, S., Skirpan, A., Lunde, C., Wu, X., Kellogg, E. *et al.* (2007) *Barren inflorescence2* encodes a co-ortholog of the PINOID serine/threonine kinase and is required for organogenesis during inflorescence and vegetative development in maize. *Plant Physiology*, **144**, 1000–1011.
- Ning, Q., Jian, Y., Du, Y., Li, Y., Shen, X., Jia, H. *et al.* (2021) An ethylene biosynthesis enzyme controls quantitative variation in maize ear length and kernel yield. *Nature Communications*, **12**, 5832.
- Pei, Y., Deng, Y., Zhang, H., Zhang, Z., Liu, J., Chen, Z. *et al.* (2022) *EAR APICAL DEGENERATION1* regulates maize EAR development by maintaining malate supply for apical inflorescence. *The Plant Cell*, **34**, 2222–2241.
- Phillips, K.A., Skirpan, A.L., Liu, X., Christensen, A., Slewinski, T.L., Hudson, C. *et al.* (2011) *Vanishing tassel2* encodes a grass-specific tryptophan aminotransferase required for vegetative and reproductive development in maize. *The Plant Cell*, **23**, 550–566.
- Ross, J.J., O'Neill, D.P., Wolbang, C.M., Symons, G.M. & Reid, J.B. (2001) Auxin-gibberellin interactions and their role in plant growth. *Journal of Plant Growth Regulation*, **20**, 336–353.
- Salse, J., Bolot, S., Throude, M., Jouffe, V., Piegu, B., Quraishi, U.M. *et al.* (2008) Identification and characterization of shared duplications between rice and wheat provide new insight into grass genome evolution. *The Plant Cell*, **20**, 11–24.
- Schindelin, J., Rueden, C.T., Hiner, M.C. & Eliceiri, K.W. (2015) The ImageJ ecosystem: an open platform for biomedical image analysis. *Molecular Reproduction and Development*, **82**, 518–529.
- Schnable, J.C., Springer, N.M. & Freeling, M. (2011) Differentiation of the maize subgenomes by genome dominance and both ancient and ongoing gene loss. *Proceedings of the National Academy of Sciences of the United States of America*, **108**, 4069–4074.
- Šimura, J., Antoniadi, I., Široká, J., Tarkowská, D., Strnad, M., Ljung, K. *et al.* (2018) Plant hormonomics: multiple phytohormone profiling by targeted metabolomics. *Plant Physiology*, **177**, 476–489.
- Vollbrecht, E. & Schmidt, R.J. (2009) Development of the Inflorescences. In: *Handbook of maize: its biology*. New York: Springer, pp. 13–40.
- Wei, F., Coe, E., Nelson, W., Bharti, A.K., Engler, F., Butler, E. *et al.* (2007) Physical and genetic structure of the maize genome reflects its complex evolutionary history. *PLoS Genetics*, **3**, e123.
- Xiao, Y., Tong, H., Yang, X., Xu, S., Pan, Q., Qiao, F. *et al.* (2016) Genome-wide dissection of the maize ear genetic architecture using multiple populations. *New Phytologist*, **210**, 1095–1106.
- Xu, C., Zhang, H., Sun, J., Guo, Z., Zou, C., Li, W.X. *et al.* (2018) Genome-wide association study dissects yield components associated with low-phosphorus stress tolerance in maize. *Theoretical and Applied Genetics*, **131**, 1699–1714.
- Yi, Q., Liu, Y., Hou, X., Zhang, X., Li, H., Zhang, J. *et al.* (2019) Genetic dissection of yield-related traits and mid-parent heterosis for those traits in maize (*Zea mays* L.). *BMC Plant Biology*, **19**, 392.
- Yoo, S.D., Cho, Y.H. & Sheen, J. (2007) *Arabidopsis* mesophyll protoplasts: a versatile cell system for transient gene expression analysis. *Nature Protocols*, **2**, 1565–1572.
- Zhang, D., Zhou, G., Liu, B., Kong, Y., Chen, N., Qiu, Q. *et al.* (2011) *HCF243* encodes a chloroplast-localized protein involved in the D1 protein stability of the *Arabidopsis* photosystem II complex. *Plant Physiology*, **157**, 608–619.
- Zhao, Y. (2010) Auxin biosynthesis and its role in plant development. *Annual Review of Plant Biology*, **61**, 49–64.
- Zhou, B., Zhou, Z., Ding, J., Zhang, X., Mu, C., Wu, Y. *et al.* (2018) Combining three mapping strategies to reveal quantitative trait loci and candidate genes for maize ear length. *Plant Genome*, **11**, 107.